Neuron, Vol. 42, 401–410, May 13, 2004, Copyright ©2004 by Cell Press

Subunit Configuration of Heteromeric Cone Cyclic Nucleotide-Gated Channels

Changhong Peng,[1] Elizabeth D. Rich,[1] and Michael D. Varnum[1,2,*]
[1]Department of Veterinary and Comparative Anatomy, Pharmacology, and Physiology
[2]Program in Neuroscience and Center for Integrated Biotechnology
Washington State University
P.O. Box 646520
Pullman, Washington 99164

Summary

Cone photoreceptor cyclic nucleotide-gated (CNG) channels are thought to be tetrameric assemblies of CNGB3 (B3) and CNGA3 (A3) subunits. We have used functional and biochemical approaches to investigate the stoichiometry and arrangement of these subunits in recombinant channels. First, tandem dimers of linked subunits were used to constrain the order of CNGB3 and CNGA3 subunits; the properties of channels formed by B3/B3+A3/A3 dimers, or A3/B3+B3/A3 dimers, closely resembled those of channels arising from B3+A3 monomers. Functional markers in B3/B3 (or A3/A3) dimers confirmed that both B3 subunits (and both A3 subunits) gained membership into the pore-forming tetramer and that like subunits were positioned adjacent to each other. Second, chemical crosslinking and co-immunoprecipitation studies using epitope-tagged monomer subunits both demonstrated the presence of two CNGB3 subunits in cone channels. Together, these data support a preferred subunit arrangement for cone CNG channels (B3-B3-A3-A3) that is distinct from the 3A:1B configuration of rod channels.

Introduction

Cyclic nucleotide-gated (CNG) channels are vital to the signaling pathways that convert sensory stimuli in retinal photoreceptors (Burns and Baylor, 2001) and olfactory receptor neurons (Zufall and Munger, 2001) into electrical signals that are processed as visual or olfactory information. In these cell types, CNG channels signal the change in intracellular concentration of cyclic nucleotide that accompanies receptor activation by closing or opening their ion conduction pathways, leading to membrane hyperpolarization or depolarization, respectively.

Similar to their voltage-gated potassium channel relatives (Jan and Jan, 1990), CNG channels are tetrameric proteins (Gordon and Zagotta, 1995; Liu et al., 1996; Varnum and Zagotta, 1996), with each subunit including an intracellular cyclic nucleotide binding domain; binding of cGMP or cAMP to these sites is coupled to opening of the channel pore (Kaupp and Seifert, 2002; Matulef and Zagotta, 2003). In mammals, six genes are known to encode CNG channel subunits: CNGA1, CNGA2, CNGA3, CNGA4, CNGB1, and CNGB3 (Bradley et al., 2001a; Richards and Gordon, 2000). Most native channels are thought to be heteromeric proteins formed by two or three of these subunit types. While CNGA1, CNGA2, and CNGA3 subunits can form functional homomeric channels, co-assembly with one or more of the other, "modulatory" subunits is necessary to generate channels with properties optimized for the roles these proteins play in their specialized cells.

The cell type-specific expression of CNG channel genes helps determine the make-up of the sensory transduction channels. In olfactory receptor neurons, channels are composed of CNGA2, CNGA4, and CNGB1b subunits (Bonigk et al., 1999; Bradley et al., 1994; Dhallan et al., 1990; Liman and Buck, 1994; Ludwig et al., 1990; Sautter et al., 1998). The CNGA4 and CNGB1b subunits are critical for enhancing the sensitivity of these proteins to Ca^{2+}-calmodulin (CaM) regulation (Bradley et al., 2001b; Munger et al., 2001), an important feedback signal involved in olfactory adaptation (Kurahashi and Menini, 1997). Rod photoreceptor CNG channels are made up of CNGA1 (Kaupp et al., 1989) and CNGB1 (Chen et al., 1993), while cone photoreceptor CNG channels are comprised of CNGA3 (Bonigk et al., 1993) and CNGB3 (Gerstner et al., 2000) subunits. For both rod and cone CNG channels, the CNGB1 and CNGB3 subunits tune the properties of the heteromeric channels formed with CNGA1 or CNGA3 subunits, respectively; this includes conferring sensitivity to regulation by Ca^{2+}-CaM (Chen et al., 1994; Peng et al., 2003a).

Understanding the specific mechanisms and subunit interactions involved in activation and regulation of heteromeric CNG channels requires knowledge about how these proteins are assembled and arranged as heteromultimers. Several recent studies have examined the stoichiometry of heteromeric rod CNG channels formed by assembly of CNGA1 and CNGB1 subunits, suggesting that these tetrameric proteins contain three A1 subunits and one B1 subunit (Figure 1A; Weitz et al., 2002; Zheng et al., 2002; Zhong et al., 2002). In addition, with the identification of a putative trimerization domain in CNGA3, these findings were extrapolated to describe the likely stoichiometry of cone CNG channels (Zhong et al., 2002). This idea, however, has not been explicitly tested for heteromeric channels containing CNGB3 subunits.

Here we describe experiments investigating the stoichiometry and arrangement of human CNGB3 and CNGA3 subunits in heteromeric channels. We have applied both functional and biochemical approaches, providing evidence that cone CNG channels exhibit a two plus two stoichiometry of CNGB3 and CNGA3 subunits, with like subunits arranged adjacent to each other. First, channels formed by heterologous expression of B3/B3+A3/A3 tandem dimers, or of B3/A3+A3/B3 dimers, closely resembled those of channels arising from co-expression of B3 and A3 monomers, while channels generated with B3/A3 or A3/B3 dimers did not. Second, limited chemical crosslinking of intact oocytes expressing epitope-tagged subunits revealed a product exhib-

*Correspondence: varnum@wsu.edu

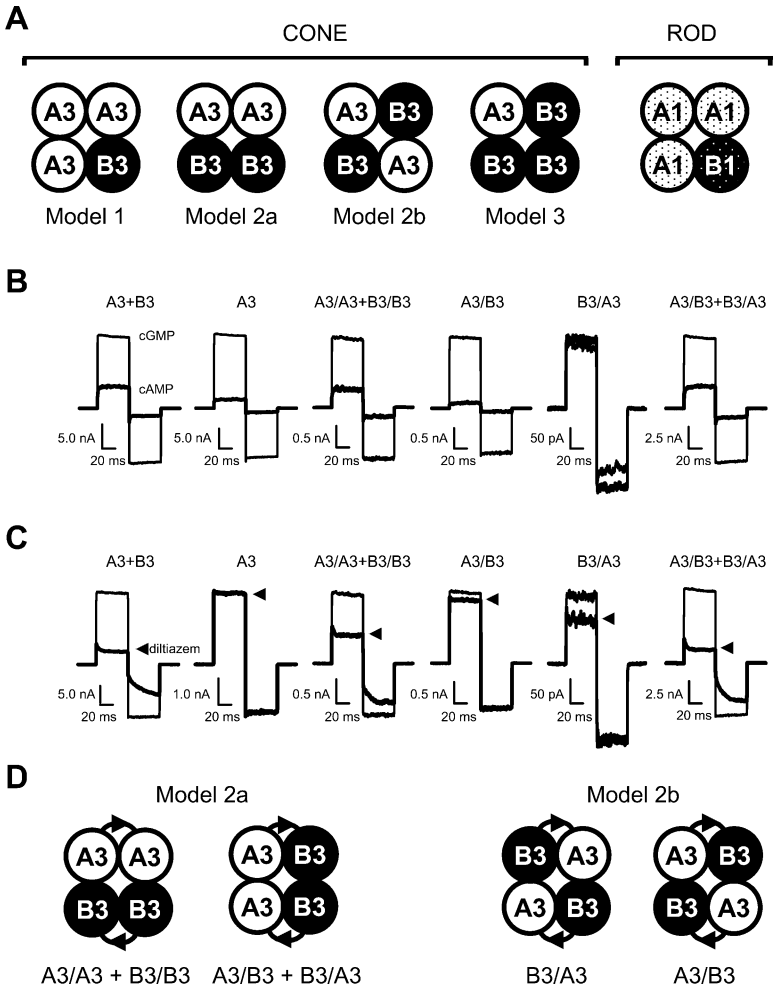

Figure 1. Representative Current Traces for Channels Formed after Expression of Different Wild-Type Tandem Dimers in *Xenopus* Oocytes

(A) Possible subunit arrangements for heteromeric cone photoreceptor CNG channels. Heteromeric rod CNG channel configuration (Weitz et al., 2002; Zheng et al., 2002; Zhong et al., 2002) is shown at right.

(B) Current traces after activation by 1 mM cGMP or 10 mM cAMP (bold). The traces were elicited by voltage steps from a holding potential of 0 mV to +80 mV, then to −80 mV and 0 mV. Leak currents in the absence of cyclic nucleotide were subtracted for all recordings. For a given tandem dimer, *x*/*y*, *x* is the NH_2-terminal or leading subunit and *y* is the COOH-terminal or trailing subunit.

(C) Currents elicited by 1 mM cGMP in the absence and presence (bold) of 25 μM L-*cis*-diltiazem with the same protocol described in (B).

(D) Expected subunit arrangements arising from head to tail assembly of indicated tandem dimers. Arrows designate orientation of linkage from NH_2- to COOH-terminal subunits.

iting a molecular weight twice that of B3 monomers, consistent with the presence of two B3 subunits in mature channels. Third, co-immunoprecipitation studies with differentially tagged subunits indicated that two CNGB3 subunits associated together, in contrast to rod CNGB1 subunits that did not co-assemble. All three of these independent approaches support a B3-B3-A3-A3 subunit arrangement in heteromeric cone CNG channels.

Results

Tetrameric CNG channels composed of cone photoreceptor CNGB3 and CNGA3 subunits can theoretically assemble with three possible subunit stoichiometries and four possible configurations around the central pore (Figure 1A). Subunit assembly and arrangement might occur in some preferred manner, dictated by specific interactions among subunit-association domains, or it could be a stochastic process. In the latter case, random subunit assembly and the corresponding properties of the resulting channels would be expected to be very sensitive to the ratio of expressed CNGB3 and CNGA3 subunits.

We expressed human CNGB3 and CNGA3 subunits together in *Xenopus* oocytes and recorded macroscopic cGMP- and cAMP-activated currents from excised, inside-out membrane patches. As previously described (Peng et al., 2003a, 2003b), many of the fundamental properties of the heteromeric channels formed by this combination of subunits differ significantly from those of channels formed by human CNGA3 subunits alone. As shown in Figures 1B and 1C and Table 1, channels containing CNGB3 subunits exhibited an increase in fractional activation by a saturating concentration of cAMP compared with saturating cGMP, altered steady-state rectification ($I_{max,+80\ mV}/I_{max,-80\ mV}$) in saturating concentrations of cGMP or cAMP, increased sensitivity to block by L-*cis*-diltiazem, and an increase in the apparent affinity for cAMP and decrease in apparent affinity for cGMP. The electrophysiological behavior of CNGB3 plus CNGA3 channels (Gerstner et al., 2000; Peng et al., 2003a) suggests that this combination of subunits may represent the composition of the native cone photoreceptor CNG channel (Hackos and Korenbrot, 1997; Haynes and Yau, 1985; Haynes, 1992; Picones and Korenbrot, 1992).

To determine whether CNGB3 and CNGA3 subunits combine at random to form heteromeric channels or instead assemble with a preferred stoichiometry, we examined the functional properties of heteromeric channels arising from co-injection of mRNA for CNGB3 and

Table 1. Summary of Channel Properties for Co-expression of CNGB3 with CNGA3 at Varying Ratios

	cGMP		cAMP				
	$K_{1/2}$ (μM)	*h*	$K_{1/2}$ (μM)	*h*	I_{cAMP}/I_{cGMP}	$I_{diltiazem}/I$	I_{cGMP} +80 mV/−80 mV
A3	10.9 ± 2.3 (32)	2.1 ± 0.3	1168 ± 214 (23)	1.3 ± 0.4	0.15 ± 0.05 (31)	0.94 ± 0.02 (5)	1.50 ± 0.21
1:10 B3 + A3	16.2 ± 2.8 (18)	2.2 ± 0.2	988 ± 155 (12)	1.5 ± 0.2	0.23 ± 0.10 (19)	0.54 ± 0.06 (4)	1.27 ± 0.14
1:5 B3 + A3	13.6 ± 2.6 (16)	1.8 ± 0.2	752 ± 252 (14)	1.3 ± 0.2	0.35 ± 0.09 (15)	0.44 ± 0.18 (5)	1.22 ± 0.15
1:1 B3 + A3	14.2 ± 1.3 (7)	1.9 ± 0.2	870 ± 211 (7)	1.3 ± 0.1	0.34 ± 0.05 (8)	0.27 ± 0.08 (4)	1.23 ± 0.08
5:1 B3 + A3	16.0 ± 1.9 (8)	1.8 ± 0.2	890 ± 122 (7)	1.4 ± 0.1	0.32 ± 0.07 (9)	0.35 ± 0.10 (4)	1.28 ± 0.10
10:1 B3 + A3	14.3 ± 1.9 (5)	1.8 ± 0.1	964 ± 130 (5)	1.4 ± 0.1	0.23 ± 0.03 (5)	0.45 ± 0.09 (4)	1.40 ± 0.08

CNGA3 at varying ratios. Similar to recombinant rod (He et al., 2000; Shammat and Gordon, 1999) and olfactory (Shapiro and Zagotta, 2000) heteromeric CNG channels, most of the fundamental features of heteromeric cone CNG channels were relatively invariant over a wide range of subunit expression ratios (Table 1). These results indicate that cone CNG channels probably assemble in some preferred manner, with a consistent stoichiometry of CNGB3 and CNGA3 subunits.

Tandem Dimer Expression Suggests B3-B3-A3-A3 Subunit Configuration

We employed concatenated cDNA constructs encoding tandemly linked dimers of CNGB3 and/or CNGA3 subunits to specify the number and arrangement of subunits in functional channels and to determine which arrangements are best able to form channels with properties matching those of heteromeric channels assembled from monomeric CNGB3 and CNGA3. Tetrameric channels can form by assembly of two of these tandem dimers. The linker between two subunits was chosen to be flexible and short, to minimize the effect of the linkage on the properties of the resulting channels but also to constrain linked subunits to be adjacent within the tetramer. Assuming head to tail assembly of two dimers, the predicted subunit arrangement for some of the expressed tandem dimers or dimer combinations is depicted in Figure 1D. Co-expression of A3/A3 with B3/B3 dimers, or of A3/B3 with reciprocal B3/A3 dimers, is expected to permit the formation of heteromeric channels with like subunits positioned adjacent to each other (Figures 1A and 1D, Model 2a). In contrast, expression of A3/B3 or B3/A3 dimers alone is expected to favor formation of heteromeric channels with like subunits diagonally opposed (Figures 1A and 1D, Model 2b).

As expected, expression of B3/B3 dimers alone did not give rise to functional CNG channels (data not shown). Co-expression of B3/B3 with A3/A3 dimers, or of B3/A3 with A3/B3 dimers, led to the formation of channels that exhibited properties that closely resembled those of channels assembled from CNGB3 and CNGA3 monomers (Figures 1B, 1C, and 2A–2E). Current records at +80 mV and −80 mV in saturating ligand concentrations showed that both B3/B3+A3/A3 channels and B3/A3+A3/B3 channels displayed the characteristic high relative cAMP efficacy compared to cGMP, altered steady-state rectification in cAMP and cGMP, and sensitivity to block by L-*cis*-diltiazem that is associated with heteromeric cone CNG channels (Figures 1B, 1C, and 2A–2C). In addition, the apparent affinities of these channels for cGMP or cAMP were similar to those observed for channels formed by CNGB3 plus CNGA3 monomers (Figures 2D and 2E).

In contrast, channels formed by individual expression of either A3/B3 or B3/A3 dimers displayed properties dramatically different from those of channels arising from CNGB3 plus CNGA3 monomers. For all parameters examined, channels formed by A3/B3 dimers resembled the homomeric channels fashioned from CNGA3 monomers or A3/A3 dimers (Figures 1B, 1C, and 2). Channel properties observed after expression of B3/A3 dimers were unlike those of heteromeric CNGB3+CNGA3 channels, homomeric CNGA3 channels, or the channels formed by A3/B3 dimers. In addition, the level of functional expression for B3/A3 dimers was very low (Figure 2F). Thus, only when expression of the tandem dimers was expected to favor the Model 2a configuration (A3-A3-B3-B3, Figures 1A and 1D) were the properties of the resulting channels in close agreement with those of heteromeric channels formed by CNGB3 plus CNGA3 monomers.

From previous studies using tandem-dimer constructs, there is evidence indicating that the trailing (COOH-terminal) subunit of a tandem dimer can sometimes be excluded from the pore-forming tetramer; this is thought to be more likely to occur if inclusion of that subunit is adverse to optimal channel formation (Liman et al., 1992; McCormack et al., 1992; Shapiro and Zagotta, 1998). The dissimilar behavior of A3/B3 versus B3/A3 tandem dimers expressed individually, and the correspondence between the currents observed with A3/B3 dimers and those of A3/A3 homomeric channels, suggests that at least for A3/B3 expression this might be the case. To confirm that both subunits of A3/A3 and B3/B3 tandem homodimers were equally competent for participation in the formation of heteromeric channels and to test for unequal numbers of CNGA3 and CNGB3 subunits in the tetramer (Models 1 and 3, Figure 1A), reciprocal dimers were engineered such that either the leading or trailing subunit contained a marker mutation expected to alter the functional properties of the expressed channels when that marked subunit is incorporated into tetramers. Each of these A3/A3 or B3/B3 heterodimer constructs was co-expressed with CNGB3 or CNGA3, respectively. The basic properties of the channels formed under these conditions are predicted to be identical to each other if both subunits of the dimer gain membership into the pore-forming tetramer (as in Figures 3A and 4A, prediction for Model 2a) but different if exclusion of the trailing subunit is favored (Figures 3A and 4A, predictions for Models 1, 2b, and 3).

To add a functional tag to CNGA3 subunits in tandem dimers, we used mutation of a conserved aspartic acid

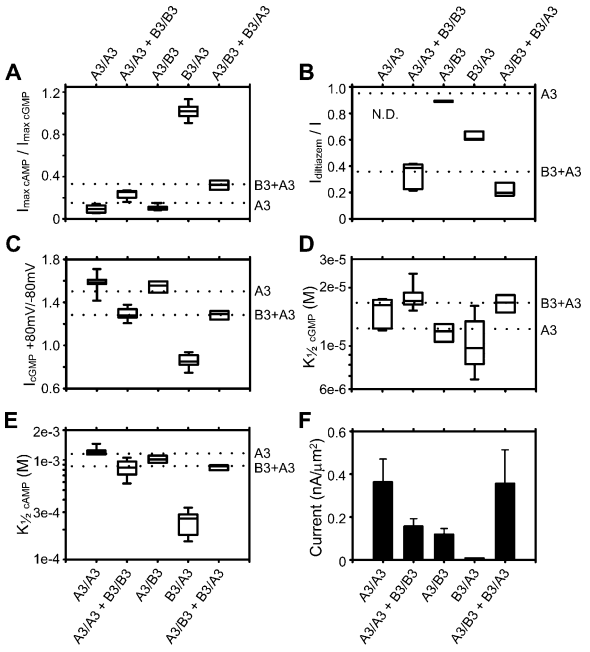

Figure 2. Functional Properties of Channels Formed by Expression of Wild-Type Tandem-Dimer Constructs

(A) Ratio of the current elicited by saturating concentrations of cAMP (10 mM) and cGMP (1 mM) at +80 mV (n = 4–9). The vertical line within the box indicates the median of the data; boxes show the 25th and 75th percentiles, and whiskers show the 5th and 95th percentiles. Dotted lines indicate the corresponding mean values from 5:1 expression ratio for B3+A3, or A3 in Table 1.

(B) Block by 25 μM L-*cis*-diltiazem at +80 mV in the presence of 1 mM cGMP, normalized to the current in the absence of diltiazem (n = 3–5).

(C) Steady-state rectification (+80/−80 mV) in 1 mM cGMP (n = 4–9).

(D) Apparent affinity for cGMP, from fits of Hill equation to dose-response data (n = 4–10).

(E) Apparent affinity for cAMP, from fits of Hill equation to dose-response data (n = 4–9).

(F) Maximum patch current density (mean ± SE; n = 4–11), within the same experimental group, calculated after estimating patch area, A (in μm^2), from the initial pipette resistance, R, using the following equation: $A = 12.6 \times (1/R + 0.018)$ (Sakmann and Neher, 1983).

residue in the cyclic nucleotide binding domain of the CNGA3 subunit (D609; corresponding to D604 in bovine CNGA1) that has been shown previously to be crucial for ligand selectivity of CNG channels (Varnum et al., 1995a). Mutation of the negatively charged side chain at this position, in all or in two of the four channel subunits, decreases the effectiveness of cGMP to promote channel opening while enhancing the ability of cAMP to activate the channels (Varnum et al., 1995a; Varnum and Zagotta, 1996). For homomeric CNGA3 channels, the mutation applied in this study (D609K) caused an approximately 20-fold decrease in apparent affinity for cGMP (Figures 3B and 3C). As expected, channels formed by expression of individual A3/A3 dimers with the D609K mutation (*) in the leading (A3*/A3) or trailing (A3/A3*) subunit of the dimer generated channels that exhibited a $K_{1/2}$ for activation by cGMP that was intermediate between channels containing all wild-type or all mutant subunits. Similarly, co-expression of CNGB3 subunits with A3*/A3 or A3/A3* dimers led to the formation of channels that displayed apparent affinities for cGMP intermediate between CNGB3-containing heteromeric channels with all wild-type or all mutant CNGA3 subunits (Figures 3B and 3C). In addition, B3+A3*/A3 channels were indistinguishable from B3+A3/A3* channels for this parameter. To confirm that these subunit combinations formed heteromeric channels, we also tested their sensitivity to block by L-*cis*-diltiazem. B3+A3*/A3 channels and B3+A3/A3* channels were both readily blocked by L-*cis*-diltiazem (Figure 3D). In addition, B3+A3*/A3 channels and B3+A3/A3* channels exhibited the elevated fractional activation by saturating cAMP compared to cGMP that is characteristic of heteromeric CNGB3+CNGA3 channels (Figure 3E). Together, these results strongly suggest that heteromeric cone CNG channels contain at least two CNGA3 subunits and that the CNGA3 subunits are arrayed adjacent to each other in the tetramer (Figure 3A, prediction for Model 2a).

To address the question of the number of CNGB3 subunits in heteromeric channels, we used a mutation in the S6 membrane-spanning domain of CNGB3 that has been linked to complete achromatopsia in humans (Kohl et al., 2000; Sundin et al., 2000). Recently, we have characterized the functional consequences of this mutation (S435F) for heteromeric channels (Peng et al., 2003b). The S435F mutation in CNGB3 increases the apparent affinity of heteromeric channels for both cAMP and cGMP, decreases the steady-state outward rectification in a saturating concentration of cAMP, reduces the single channel conductance, and substantially lowers the sensitivity of the channels to block by L-*cis*-diltiazem (Peng et al., 2003b). B3/B3 dimers were constructed with the S435F marker (*) in either the leading (B3*/B3) or trailing (B3/B3*) subunit of the dimer. As shown in Figure 4A, different models for the number of B3 subunits in cone CNG channels make unique predictions about the behavior of channels formed with B3*/B3 or B3/B3* dimers. If the preferred number of B3 subunits in the tetramer is two, then both subunits of the dimer should incorporate with equal efficiency into tetrameric channels (Figure 4A, prediction for Model 2a). In this case, the functional properties of channels formed with the reciprocal B3*/B3 or B3/B3* dimers should be similar, and the behavior of both should be intermediate between channels formed with wild-type (B3/B3) or mutant (B3*/B3*) homodimers. If the preferred number of B3 subunits in the tetramer is one, then the resulting channel behavior will be highly dependent upon which B3 subunit, mutant or wild-type, is in the leading (NH_2-terminal) position (Figure 4A, prediction for Model 1).

For activation of these channels by cAMP, the apparent affinities exhibited by the reciprocal B3*/B3 or B3/B3* dimers co-expressed with A3/A3 were similar to each other and intermediate between those of channels formed with B3/B3 or B3*/B3* homodimers (Figures 4B and 4C). Likewise, steady-state rectification of currents in saturating cAMP was also indistinguishable for B3*/B3 or B3/B3* dimers and intermediate between that of the respective homodimers (Figure 4D). Similar results were observed with co-expression of the various B3/B3 dimers with A3 monomers (data not shown). Finally, $I_{max,cAMP}/I_{max,cGMP}$ for mutant B3/B3 dimers co-expressed with A3/A3 was significantly higher than that observed

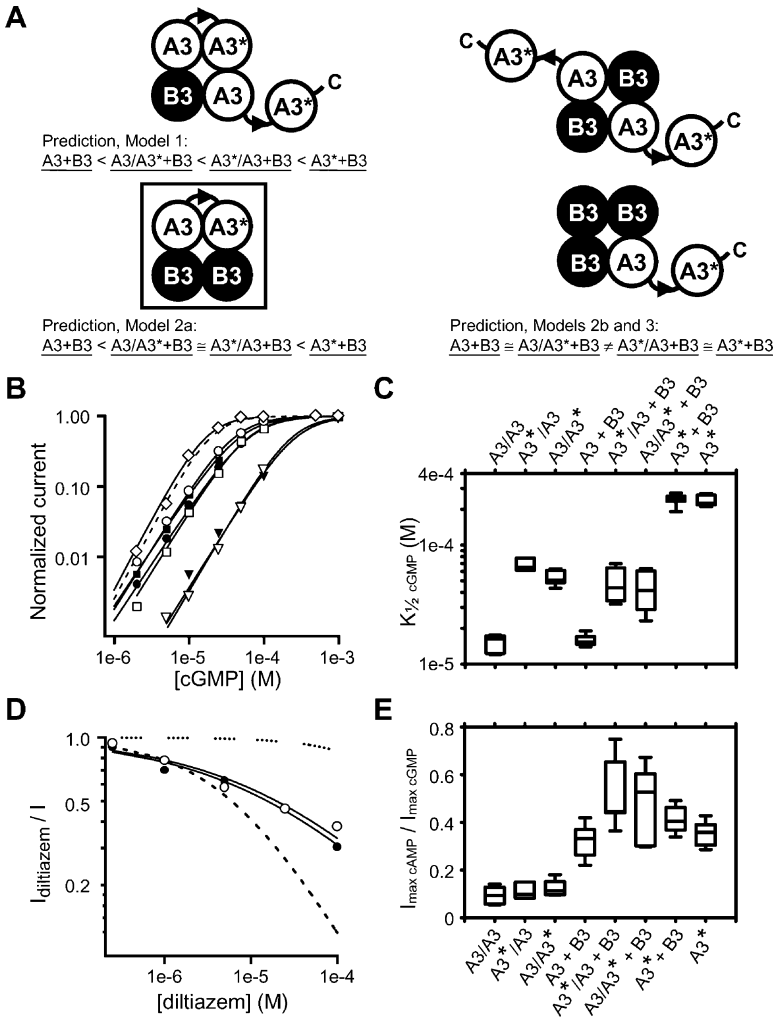

Figure 3. Leading and Trailing Subunits of A3/A3 Dimers Both Incorporate Efficiently into Heteromeric Channels

(A) Possible scenarios for exclusion of the COOH-terminal (trailing) A3 subunit from pore-forming tetramer, with associated model predictions for mutant A3/A3 heterodimers. A3* represents A3-D609K subunits in all panels.

(B) Representative dose-response relationships for channel activation by cGMP at +80 mV. Continuous curves represent fits of the dose-response relation to the Hill equation. For A3/A3 channels (open diamond), $K_{1/2}$ = 17 μM and h = 2.0; for A3*/A3 channels (open square), $K_{1/2}$ = 63 μM and h = 1.7; for A3/A3* channels (closed square), $K_{1/2}$ = 48 μM and h = 1.6; for A3*/A3+B3 channels (open circle), $K_{1/2}$ = 41 μM and h = 1.7; for A3/A3* +B3 channels (closed circle), $K_{1/2}$ = 65 μM and h = 1.6. For channels formed by co-expression of monomers of B3 and A3 (dashed line), $K_{1/2}$ = 20 μM and h = 2.0; for co-expression of monomers of A3* and B3 (open inverted triangle), $K_{1/2}$ = 240 μM and h = 1.8; for channels formed by A3* (closed inverted triangle) alone, $K_{1/2}$ = 271 μM and h = 1.7.

(C) Apparent affinity for cGMP from fits of the Hill equation (n = 4–9).

(D) Representative dose-response relationships for block by L-*cis*-diltiazem at +80 mV in the presence of 1 mM cGMP of A3/A3*+B3 (closed circle) and A3*/A3+B3 (open circle) channels. Continuous curves represent fits of the dose-response relation to the Hill equation in the form: $I_{diltiazem}/I = (K_{1/2}{}^h/(K_{1/2}{}^h + [\text{diltiazem}]^h))$. For A3/A3*+B3, $K_{1/2}$ = 16 μM and h = 0.43; for A3*/A3+B3, $K_{1/2}$ = 19 μM and h = 0.43. For channels formed by co-expression of monomers of B3 and A3 (dashed line), $K_{1/2}$ = 6 μM and h = 0.7; for homomeric A3 channels (dotted line), $K_{1/2} >> 100$ μM.

(E) Ratio of currents elicited by saturating concentrations of cAMP (10 mM) and cGMP (1 mM) at +80 mV (n = 3–9).

for A3/A3 or A3 homomeric channels, confirming that the channels studied here were largely heteromeric (Figure 4E). These findings together indicate that both B3 subunits of a B3/B3 dimer gain membership into the pore-forming tetramer, suggesting that cone CNG channels contain two B3 subunits and that like subunits are positioned adjacent to each other (Figure 4A, prediction for Model 2a).

Biochemical Determination of Cone Channel Stoichiometry

We used chemical crosslinking of epitope-tagged subunits to directly determine the number of each subunit in assembled heteromeric CNG channels. Crosslinking of rod CNG channel subunits has proven to be a powerful tool for investigating subunit interactions of recombinant (Matulef and Zagotta, 2002; Rosenbaum and Gordon, 2002) and native (Bauer and Drechsler, 1992; Weitz et al., 2002) channels. We focused on limited chemical crosslinking of intact oocytes in order to enhance the detection of nearest neighbor interactions in mature channels and to minimize capture of spurious or transitory interactions with other proteins. Possible stoichiometries for heteromeric channels provide specific predictions about the products arising from limited chemical crosslinking: a two plus two stoichiometry of CNGA3 and CNGB3 subunits is expected to yield all possible dimer combinations after crosslinking, while the presence of only one CNGA3 subunit or one CNGB3 subunit in the tetramer should lead to an absence of crosslinked A3-A3 or B3-B3 dimers, respectively. To calibrate the sizes for crosslinked CNGA3 subunits, cell lysates obtained from oocytes expressing FLAG-tagged CNGA3 (FLAG-A3) alone were subjected to crosslinking, and the resulting protein products were separated by SDS-PAGE and detected by Western blotting (Figure 5A). Monomers of FLAG-A3 exhibited a molecular weight of 73 ± 2 kDa; presumptive crosslinked dimer and trimer species had molecular weights of 149 ± 4 and 219 ± 4, respectively (n = 3). In addition, an even larger species was evident, probably representing crosslinked tetramers of CNGA3 subunits.

Limited chemical crosslinking was also applied to oocytes expressing FLAG-CNGB3 (FLAG-B3) with FLAG-A3 subunits. For these experiments, application of the membrane impermeant, noncleavable crosslinking

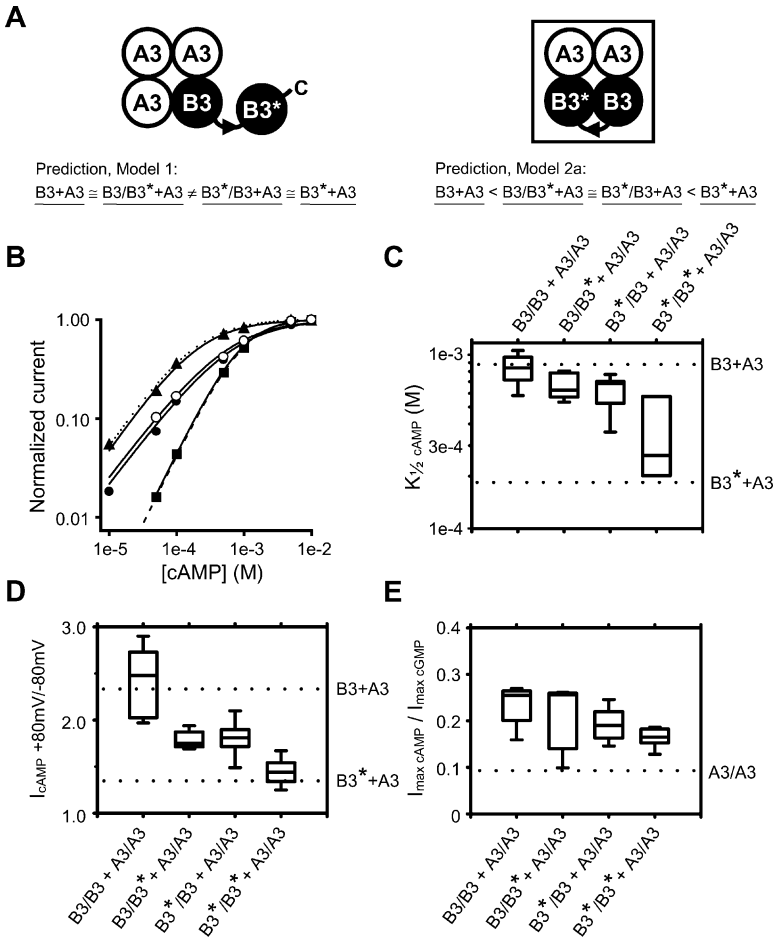

Figure 4. Leading and Trailing Subunits of B3/B3 Dimers Both Incorporate Efficiently into Heteromeric Channels

(A) Possible arrangements and model predictions for mutant B3/B3 heterodimers. B3* represents B3-S435F in all panels.

(B) Representative dose-response relationships for channel activation by cAMP at +80 mV. Continuous curves represent fits of the dose-response relation to the Hill equation. For B3/B3+A3 channels (closed square), $K_{1/2}$ = 920 μM and h = 1.4; for B3/B3*+A3 channels (open circle), $K_{1/2}$ = 600 μM and h = 0.9; for B3*/B3+A3 channels (closed circle), $K_{1/2}$ = 680 μM and h = 0.9; for B3*/B3*+A3 channels (closed triangle), $K_{1/2}$ = 200 μM and h = 1.0. For channels formed by co-expression of monomers of B3 and A3 (dashed line), $K_{1/2}$ = 950 μM and h = 1.4; for co-expression of monomers of B3* and A3 (dotted line), $K_{1/2}$ = 180 μM and h = 1.0.

(C) Apparent affinity for cAMP from fits of the Hill equation (n = 4–8). Dotted lines indicate the mean values for channels formed by the indicated monomers.

(D) Steady-state rectification (+80/−80 mV) in 10 mM cAMP (n = 5–7).

(E) Ratio of currents elicited by saturating concentrations of cAMP (10 mM) and cGMP (1 mM) at +80 mV (n = 5–9).

agent bis[sulfosuccinimidyl]suberate (BS^3) to intact oocytes was used to target mature channels in the oocyte plasma membrane. Prior to and during crosslinking, oocytes were exposed to the membrane-permeable channel activator 8-pCPT-cGMP to potentially increase the number of accessible primary amines (Varnum et al., 1995b; Weitz et al., 2002). The crosslinking reaction was terminated and the crosslinked products were visualized by Western blotting. As shown in Figure 5B, monomeric FLAG-A3 and FLAG-B3 (95 ± 1 kDa) were visible as well as prominent bands with molecular weights corresponding to those expected for A3-A3, B3-A3 (171 ± 2) and B3-B3 (193 ± 3) crosslinked species (n = 4). The generation of these three crosslinked dimers is consistent with the presence of two CNGA3 subunits and two CNGB3 subunits in the intact channel.

The size of the presumptive B3-B3 crosslinked species (Figure 5B) appeared to be smaller than that of the A3-A3-A3 crosslinked species (Figure 5A). To verify the identity of this ~190 kDa band, we additionally examined oocytes expressing tagged CNGB3 subunits with nontagged CNGA3 subunits. Under these conditions, a B3-B3 species would be visible after in situ crosslinking but an A3-A3-A3 species would not. As expected, a prominent band with a size corresponding to that predicted for B3-B3 dimers was still evident; another band probably representing B3-A3 crosslinked subunits was also apparent (Figure 5C). These results indicate that two CNGB3 subunits are associated together at the oocyte plasma membrane.

To independently confirm that two CNGB3 subunits associate during channel assembly, we also investigated cone CNG channel intersubunit interactions using a second biochemical approach. For these experiments, we employed co-immunoprecipitation assays with differentially tagged CNGB3 (and CNGA3) subunits expressed in oocytes. As expected, FLAG-tagged CNGB3 subunits were readily co-immunoprecipitated with GFP-tagged CNGA3 subunits using an anti-GFP antibody affinity matrix (Figure 6A). Similarly, FLAG-tagged CNGB3 subunits were co-immunoprecipitated from oocyte lysates containing GFP-tagged CNGB3 subunits and nontagged CNGA3 subunits. As a control, we performed parallel experiments with the CNGB1 and CNGA1 subunits of rod photoreceptor CNG channels. While CNGB1 and CNGA1 subunits readily associated, interactions between CNGB1 subunits were not observed (Figure 6B). This finding is in agreement with recent experiments demonstrating that only one CNGB1 subunit is present in heteromeric channels formed by assembly with either CNGA1 (Weitz et al., 2002; Zheng et al., 2002; Zhong et al., 2002) or CNGA3 (Zhong et al., 2002) subunits. Together, these results demonstrate that two CNGB3 subunits are assembled together and that the number of CNGB1 or CNGB3 subunits in heteromeric channels is dissimilar.

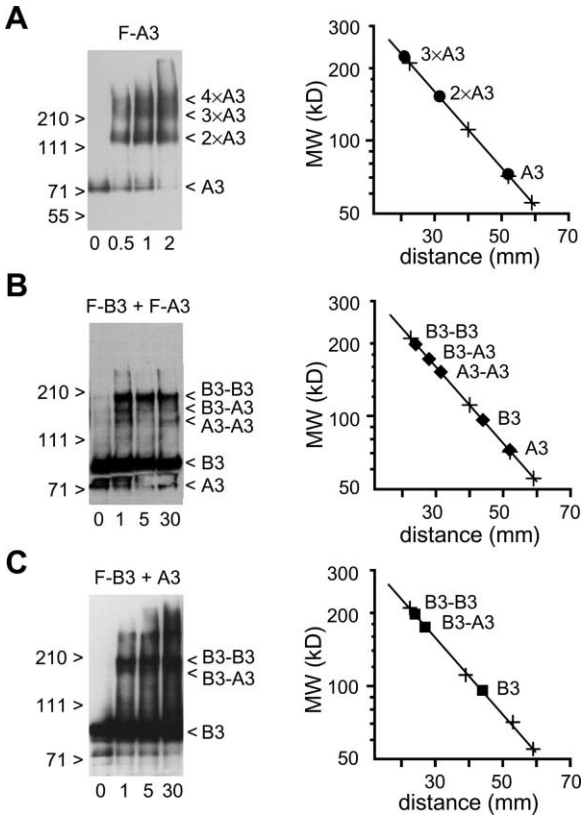

Figure 5. Limited Chemical Crosslinking Captures B3-B3 Subunit Interactions in Intact Heteromeric Channels

(A) Limited chemical crosslinking of lysates from oocytes expressing FLAG-A3 alone, using 2.5 mM gluteraldehyde for the indicated times (in minutes). Molecular weight (MW) calculations for A3 monomers, 73 ± 2; for 2×A3, 149 ± 4; for 3×A3, 219 ± 4 (n = 3) (right panel). +, molecular weight markers, as in left panel.

(B) Limited chemical crosslinking using 0.5 mM BS^3 of intact oocytes expressing FLAG-B3 and FLAG-A3 for the indicated times. Right panel shows the MW calculations for representative experiment. For B3 monomers, 95 ± 1; for B3-A3, 171 ± 2; for B3-B3, 193 ± 3 (n = 4).

(C) Crosslinking as in (B) of intact oocytes expressing FLAG-B3 and nontagged A3.

Discussion

In this study, we have used several independent approaches to show that the preferred configuration of CNGB3 and CNGA3 subunits in cone CNG channels is B3-B3-A3-A3. This proposed stoichiometry and arrangement is supported by expression studies using tandem-dimer constructs, which indicate that like subunits are positioned adjacent to each other in a two plus two array. In addition, co-immunoprecipitation experiments as well as chemical crosslinking of CNGB3 subunits in mature channels strongly imply that two CNGB3 subunits assemble together in these heteromeric channels. Other studies using cell surface expression of GFP-tagged CNGB3 or CNGA3 subunits to monitor cone CNG channel assembly indicate that heteromeric channel formation may be favored over homomeric channel assembly (Peng et al., 2003b). These results provide evidence for preferred rather than stochastic assembly of CNGB3 and CNGA3 subunits.

The failure of channels formed by B3/A3 or A3/B3 dimers to recapitulate the essential properties of channels generated by co-injection of mRNA encoding CNGB3 and CNGA3 monomers, along with the dissimilar behavior of the reciprocal B3/A3 and A3/B3 dimers, provides evidence against a A3-B3-A3-B3 arrangement of subunits for cone CNG channels. In addition, results for B3/A3 dimer expression suggest that these channels can be constrained to adopt an unfavorable subunit configuration but that they are inefficiently expressed and their properties do not resemble those of channels created by unfettered assembly of CNGB3 and CNGA3 monomers. Furthermore, the aberrant behavior of channels formed by B3/A3 dimers indicates that the spatial arrangement of subunits within the heterotetramer can have a profound effect on channel function, as is the case for homomeric channels formed by mixtures of wild-type and mutant subunits (Gordon and Zagotta, 1995; Liu et al., 1996, 1998; Varnum and Zagotta, 1996).

Comparison of findings presented in this paper with recent studies of heteromeric channels containing CNGB1 subunits (Weitz et al., 2002; Zheng et al., 2002; Zhong et al., 2002) suggests that the identity of the β subunit (CNGB1 or CNGB3) is an important determinant for heteromeric channel assembly and arrangement. While results presented here for CNGA1 plus CNGB1 channels (Figure 6B) are consistent with the proposed three CNGA1 to one CNGB1 rod channel stoichiometry (Weitz et al., 2002; Zheng et al., 2002; Zhong et al., 2002), our results for CNGA3 plus CNGB3 channels argue against the generalization of the 3A:1B model to channels containing CNGB3 subunits (Zhong et al., 2002, 2003). These latter studies (Zhong et al., 2002, 2003) investigated intersubunit interactions using channel fragments rather than intact subunits, made functional measurements of CNGB1- but not CNGB3-containing channels, and determined the relative amounts of CNGA1 and CNGB1 subunits in native channels purified from rod photoreceptor membranes. Based on results with CNGB3-containing heteromeric channels and biochemical studies using intact CNGB3 and CNGA3 subunits, we propose instead that rod and cone channels are highly specialized, even at the level of subunit stoichiometry. Although rod and cone photoreceptors have similar basic components and signaling strategies, they express related but distinct genes for many of the proteins involved in phototransduction, and their responses differ in sensitivity and kinetics as well as in the rate, range, and mechanisms of adaptation (Fain et al., 2001; Frings et al., 1995; Miller et al., 1994; Picones and Korenbrot, 1995; Rebrik and Korenbrot, 2004). Native cone CNG channel specialization may require two rather than one CNGB3 subunit for optimal channel activity and regulation.

Subunit-specific assembly rules are thought to be important also for the formation of other heteromeric channels, including potassium channels (Salkoff et al., 1992; Shen and Pfaffinger, 1995; Xu et al., 1995) and glutamate receptor channels (Mansour et al., 2001; Schorge and Colquhoun, 2003). The paralogous human genes encoding CNGB1 and CNGB3 subunits display approximately 60% identity in predicted amino acid sequence, excluding the extreme NH_2- and COOH-terminal regions. Sequence divergence for CNGB1 and CNGB3 is expected

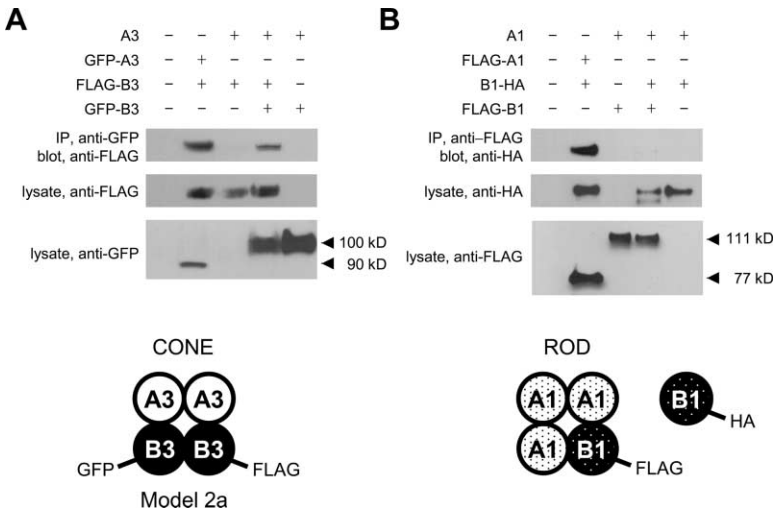

Figure 6. Co-immunoprecipitation of Differentially Tagged Subunits Suggests that Two CNGB3 Subunits Assemble Together

(A) Oocytes were microinjected with mRNA encoding the constructs indicated above. Co-immunoprecipitations were carried out using an affinity matrix with anti-GFP antibody (IP), and the resulting complexes were blotted and probed with anti-FLAG antibody (upper blot). Immunoblots of total cell lysates were probed with anti-FLAG (middle blot) or anti-GFP antibodies (lower blot). The cartoon below depicts the configuration consistent with these results and those shown above.

(B) Complementary experiment for CNGB1 + CNGA1 heteromeric channels and cartoon summary below in agreement with rod channel configuration (Weitz et al., 2002; Zheng et al., 2002; Zhong et al., 2002).

to underlie differences in subunit-association properties, and ultimately channel configuration, between rod and cone photoreceptor CNG channels. Additional experiments are needed to precisely define the structural features within CNGB3 and CNGB1 that are responsible for subunit-specific assembly and configuration.

Overall, the simplest interpretation of data presented here is that the preferred subunit arrangement of heteromeric cone CNG channels is B3-B3-A3-A3. It remains possible but unlikely that native cone channels can adopt a different configuration. Another more complicated explanation still consistent with our results is that cone CNG channels form higher order complexes composed of two or more associated channels. We favor a model where energetically favorable associations between CNGB3 subunits form during subunit synthesis and assembly, and these help define the stoichiometry and arrangement of the subunits in mature cone CNG channels. This mechanism produces a channel configuration that is distinct from heteromeric rod or olfactory CNG channels containing CNGB1 instead of CNGB3 subunits. Thus, the fixed stoichiometry and arrangement of channel-forming subunits, along with the cell type-specific expression of particular CNG channel genes, may form the basis for sensory transduction channel specialization.

Experimental Procedures

Molecular Biology

The human CNGB3 clone was isolated from human retinal cDNA as previously described (Peng et al., 2003a). The coding sequence of this clone differs from the complete published sequence for human CNGB3 (Kohl et al., 2000) (AF272900) at two positions, G1789A and A1834G, representing either Taq polymerase errors or sequence polymorphisms; both changes are silent. Human CNGA3 (Yu et al., 1996) was kindly provided by Dr. K.-W. Yau. Both CNGB3 and CNGA3 were subcloned into pGEMHE (Liman et al., 1992) for heterologous expression in *Xenopus* oocytes. Mutations in CNGB3 and CNGA3 were engineered using overlapping PCR mutagenesis (Ho et al., 1989). All mutations and the fidelity of PCR-amplified cassettes were confirmed by automated DNA sequencing. For concatenated cDNA constructs, the stop codon for the leading subunit and the start codon for the trailing subunit were replaced by a short linker sequence (IAGGGGGRARLPA), combining the coding sequences for the two subunits in a single open reading frame. The gene fusion site for the trailing (COOH-terminal) subunit was at amino acid F2 for CNGB3 and D24 for CNGA3. Previous studies (Varnum and Zagotta, 1996) and results shown in this paper for A3/A3 dimers suggest that the linker has only a small effect on the activation properties of the channels. For biochemistry experiments, a 3×FLAG epitope (MDYKDHDGDYKDHDIDYKDDDDKD) was added to the amino termini of CNGA3, CNGB3, and CNGB1 at amino acids D24, L5, and D565, respectively. CNGA1-FLAG (DYKDDDDK) was tagged at the COOH terminus after T685. GFP-tags at the NH_2 termini of CNGA3 and CNGB3 were generated as previously described (Peng et al., 2003b). HA-tagged (YPYDVPDYA) human CNGB1 was a generous gift of Dr. S.E. Gordon. These changes did not obviously alter the functional properties of the channels formed by these subunits (data not shown). For oocyte expression, identical amounts of cDNA were linearized using Nhe I or Sph I, and capped cRNA was transcribed in vitro with the T-7 RNA polymerase mMessage mMachine kit (Ambion, Austin, TX). For tandem dimer constructs, the cDNA and transcribed cRNA were checked for recombination by agarose gel electrophoresis under nondenaturing or denaturing conditions, respectively. RNA concentrations and relative amounts were determined using 1D Image Analysis software (Kodak, NY) and spectrophotometry.

Electrophysiology

For functional expression studies, *Xenopus laevis* oocytes were isolated and microinjected with 5–10 ng of in vitro transcribed mRNA as described previously (Varnum et al., 1995a). Two to seven days after microinjection, patch-clamp experiments were performed in the inside-out configuration, using an Axopatch 200B amplifier (Axon Instruments) and Pulse software (HEKA Elektronik, Lambrecht, Germany). Recordings were made at 20°C to 22°C. Initial pipette resistances were 0.45–0.75 Mohm. Intracellular and extracellular solutions contained 130 mM NaCl, 0.2 mM EDTA, and 3 mM HEPES (pH 7.2). Cyclic nucleotides were added to intracellular solution as needed, and intracellular solutions were changed using an RSC-160 rapid solution changer (Molecular Kinetics, Pullman, WA). Currents in the absence of cyclic nucleotide were subtracted. Data were analyzed using Igor Pro (Wavemetrics, Lake Oswego, OR) and SigmaPlot (SPSS, Chicago, IL). Dose-response data were fitted to the Hill equation, $I/I_{max} = ([cNMP]^h/(K_{1/2}{}^h + [cNMP]^h))$, where I is the current amplitude, I_{max} is the maximum current, [cNMP] is the ligand concentration, $K_{1/2}$ is the apparent affinity for ligand, and *h* is the Hill slope. For current inhibition by L-*cis*-diltiazem, data were fit to the Hill equation in the form: $I_{diltiazem}/I = (K_{1/2}{}^h/(K_{1/2}{}^h + [diltiazem]^h))$. The data were expressed as mean ± SD unless otherwise indicated. Statistical significance was determined using a Student's t test or Mann-Whitney rank sum test (SigmaStat; SPSS), and a p value of <0.05 was considered significant.

Chemical Crosslinking

Limited chemical crosslinking was performed in situ on intact oocytes, or after homogenization of oocytes, expressing FLAG-tagged subunits. For in situ crosslinking, oocytes were washed in buffer containing 20 mM HEPES (pH 7.4), 150 mM NaCl, and 10 mM EDTA; on ice, oocytes were pre-incubated with 1 mM CPT-cGMP, and freshly prepared bis[sulfosuccinimidyl]suberate (BS^3; Pierce, Rockford, IL) was added at 0.5 mM final concentration. After the indicated times, crosslinking was stopped by addition of Tris (pH 7.5) at a final concentration of 0.2 M. For crosslinking of oocyte lysates, 2.5 mM glutaraldehyde (or BS^3) was used; crosslinking was stopped as described above. Protein samples were separated by SDS-PAGE under reducing conditions using NuPAGE Tris acetate 3%–8% gels (Invitrogen, Carlsbad, CA) and the recommended buffer system. Proteins were then transferred to nitrocellulose using the NuPAGE transfer buffer system (Invitrogen). Approximately 0.2 oocytes per lane were loaded. Proteins were detected with anti-FLAG M2 monoclonal antibody (Sigma) and SuperSignal West Dura Extended duration substrate (Pierce). The approximate molecular weights of the tagged subunits were calculated by interpolation using the linear relationship between the log of molecular weight for protein standards (SeeBlue Plus2; Invitrogen), as reported by the manufacturer for these buffer conditions, and the migration distance of the proteins.

Co-immunoprecipitation

Soluble fractions containing oocyte proteins were prepared using a protocol adapted from Rosenbaum and others (Peng et al., 2003b; Rho et al., 2000; Rosenbaum and Gordon, 2002). Briefly, oocytes were lysed in buffer containing 20 mM HEPES (pH 7.5), 150 mM NaCl, 5 mM EDTA, 0.5% Triton X-100 (Surfact-Amps X-100; Pierce, Rockford, IL), and a protease inhibitor cocktail (Roche Applied Science, Indianapolis, IN). Each 200 μL lysate (representing about 15 oocytes) was precleared, then incubated with either anti-GFP agarose beads (Vector Laboratories, Burlingame, CA) or EZview Red Anti-FLAG M2 affinity gel beads (Sigma-Aldrich, St. Louis, MO) for over 3 hr. Beads were washed four times with 400 μL lysis buffer and the precipitate was eluted with 1× NuPAGE gel-loading buffer (Invitrogen). Protein samples were separated by SDS-PAGE and immunoblotted as described above. Immunoblots of co-immunoprecipitations were probed with either anti-FLAG M2 monoclonal antibody (Sigma) or anti-HA.11 (16B12) monoclonal antibody (Covance Research Products, Berkeley, CA), and proteins were visualized using chemiluminescence.

Acknowledgments

We are grateful to L.K. Sprunger for critical reading of the manuscript and to W.N. Zagotta for many helpful suggestions. We also thank C.A. Thor for expert technical assistance, S.E. Gordon for providing the CNGB1-HA construct, and K.-W. Yau for sharing the cDNA clone for human CNGA3. This work was supported by grants from the National Eye Institute (EY12836) and the Adler Foundation to M.D.V.

Received: July 1, 2003
Revised: January 12, 2004
Accepted: April 2, 2004
Published: May 12, 2004

References

Bauer, P.J., and Drechsler, M. (1992). Association of cyclic GMP-gated channels and Na(+)-Ca(2+)-K+ exchangers in bovine retinal rod outer segment plasma membranes. J. Physiol. *451*, 109–131.

Bonigk, W., Altenhofen, W., Muller, F., Dose, A., Illing, M., Molday, R.S., and Kaupp, U.B. (1993). Rod and cone photoreceptor cells express distinct genes for cGMP-gated channels. Neuron *10*, 865–877.

Bonigk, W., Bradley, J., Muller, F., Sesti, F., Boekhoff, I., Ronnett, G.V., Kaupp, U.B., and Frings, S. (1999). The native rat olfactory cyclic nucleotide-gated channel is composed of three distinct subunits. J. Neurosci. *19*, 5332–5347.

Bradley, J., Li, J., Davidson, N., Lester, H.A., and Zinn, K. (1994). Heteromeric olfactory cyclic nucleotide-gated channels: a subunit that confers increased sensitivity to cAMP. Proc. Natl. Acad. Sci. USA *91*, 8890–8894.

Bradley, J., Frings, S., Yau, K.W., and Reed, R. (2001a). Nomenclature for ion channel subunits. Science *294*, 2095–2096.

Bradley, J., Reuter, D., and Frings, S. (2001b). Facilitation of calmodulin-mediated odor adaptation by cAMP-gated channel subunits. Science *294*, 2176–2178.

Burns, M.E., and Baylor, D.A. (2001). Activation, deactivation, and adaptation in vertebrate photoreceptor cells. Annu. Rev. Neurosci. *24*, 779–805.

Chen, T.Y., Peng, Y.W., Dhallan, R.S., Ahamed, B., Reed, R.R., and Yau, K.W. (1993). A new subunit of the cyclic nucleotide-gated cation channel in retinal rods. Nature *362*, 764–767.

Chen, T.Y., Illing, M., Molday, L.L., Hsu, Y.T., Yau, K.W., and Molday, R.S. (1994). Subunit 2 (or beta) of retinal rod cGMP-gated cation channel is a component of the 240-kDa channel-associated protein and mediates Ca(2+)-calmodulin modulation. Proc. Natl. Acad. Sci. USA *91*, 11757–11761.

Dhallan, R.S., Yau, K.W., Schrader, K.A., and Reed, R.R. (1990). Primary structure and functional expression of a cyclic nucleotide-activated channel from olfactory neurons. Nature *347*, 184–187.

Fain, G.L., Matthews, H.R., Cornwall, M.C., and Koutalos, Y. (2001). Adaptation in vertebrate photoreceptors. Physiol. Rev. *81*, 117–151.

Frings, S., Seifert, R., Godde, M., and Kaupp, U.B. (1995). Profoundly different calcium permeation and blockage determine the specific function of distinct cyclic nucleotide-gated channels. Neuron *15*, 169–179.

Gerstner, A., Zong, X., Hofmann, F., and Biel, M. (2000). Molecular cloning and functional characterization of a new modulatory cyclic nucleotide-gated channel subunit from mouse retina. J. Neurosci. *20*, 1324–1332.

Gordon, S.E., and Zagotta, W.N. (1995). Subunit interactions in coordination of Ni^{2+} in cyclic nucleotide-gated channels. Proc. Natl. Acad. Sci. USA *92*, 10222–10226.

Hackos, D.H., and Korenbrot, J.I. (1997). Calcium modulation of ligand affinity in the cyclic GMP-gated ion channels of cone photoreceptors. J. Gen. Physiol. *110*, 515–528.

Haynes, L.W. (1992). Block of the cyclic GMP-gated channel of vertebrate rod and cone photoreceptors by l–*cis*-diltiazem. J. Gen. Physiol. *100*, 783–801.

Haynes, L., and Yau, K.W. (1985). Cyclic GMP-sensitive conductance in outer segment membrane of catfish cones. Nature *317*, 61–64.

He, Y., Ruiz, M., and Karpen, J.W. (2000). Constraining the subunit order of rod cyclic nucleotide-gated channels reveals a diagonal arrangement of like subunits. Proc. Natl. Acad. Sci. USA *97*, 895–900.

Ho, S.N., Hunt, H.D., Horton, R.M., Pullen, J.K., and Pease, L.R. (1989). Site-directed mutagenesis by overlap extension using the polymerase chain reaction. Gene *77*, 51–59.

Jan, L.Y., and Jan, Y.N. (1990). A superfamily of ion channels. Nature *345*, 672.

Kaupp, U.B., and Seifert, R. (2002). Cyclic nucleotide-gated ion channels. Physiol. Rev. *82*, 769–824.

Kaupp, U.B., Niidome, T., Tanabe, T., Terada, S., Bonigk, W., Stuhmer, W., Cook, N.J., Kangawa, K., Matsuo, H., Hirose, T., et al. (1989). Primary structure and functional expression from complementary DNA of the rod photoreceptor cyclic GMP-gated channel. Nature *342*, 762–766.

Kohl, S., Baumann, B., Broghammer, M., Jagle, H., Sieving, P., Kellner, U., Spegal, R., Anastasi, M., Zrenner, E., Sharpe, L.T., and Wissinger, B. (2000). Mutations in the CNGB3 gene encoding the beta-subunit of the cone photoreceptor cGMP-gated channel are responsible for achromatopsia (ACHM3) linked to chromosome 8q21. Hum. Mol. Genet. *9*, 2107–2116.

Kurahashi, T., and Menini, A. (1997). Mechanism of odorant adaptation in the olfactory receptor cell. Nature *385*, 725–729.

Liman, E.R., and Buck, L.B. (1994). A second subunit of the olfactory

cyclic nucleotide-gated channel confers high sensitivity to cAMP. Neuron *13*, 611–621.

Liman, E.R., Tytgat, J., and Hess, P. (1992). Subunit stoichiometry of a mammalian K^+ channel determined by construction of multimeric cDNAs. Neuron *9*, 861–871.

Liu, D.T., Tibbs, G.R., and Siegelbaum, S.A. (1996). Subunit stoichiometry of cyclic nucleotide-gated channels and effects on subunit order on channel function. Neuron *16*, 983–990.

Liu, D.T., Tibbs, G.R., Paoletti, P., and Siegelbaum, S.A. (1998). Constraining ligand-binding site stoichiometry suggests that a cyclic-nucleotide-gated channel is composed of two functional dimers. Neuron *21*, 235–248.

Ludwig, J., Margalit, T., Eismann, E., Lancet, D., and Kaupp, U.B. (1990). Primary structure of cAMP-gated channel from bovine olfactory epithelium. FEBS Lett. *270*, 24–29.

Mansour, M., Nagarajan, N., Nehring, R.B., Clements, J.D., and Rosenmund, C. (2001). Heteromeric AMPA receptors assemble with a preferred subunit stoichiometry and spatial arrangement. Neuron *32*, 841–853.

Matulef, K., and Zagotta, W. (2002). Multimerization of the ligand binding domains of cyclic nucleotide-gated channels. Neuron *36*, 93–103.

Matulef, K., and Zagotta, W.N. (2003). Cyclic nucleotide-gated ion channels. Annu. Rev. Cell Dev. Biol. *19*, 23–44.

McCormack, K., Lin, L., Iverson, L., Tanouye, M., and Sigworth, F. (1992). Tandem linkage of Shaker K^+ channel subunits does not ensure the stoichiometry of expressed channels. Biophys. J. *63*, 1406–1411.

Miller, J.L., Picones, A., and Korenbrot, J.I. (1994). Differences in transduction between rod and cone photoreceptors: an exploration of the role of calcium homeostasis. Curr. Opin. Neurobiol. *4*, 488–495.

Munger, S.D., Lane, A.P., Zhong, H., Leinders-Zufall, T., Yau, K.W., Zufall, F., and Reed, R.R. (2001). Central role of the CNGA4 channel subunit in Ca^{2+}-calmodulin-dependent odor adaptation. Science *294*, 2172–2175.

Peng, C., Rich, E.D., Thor, C.A., and Varnum, M.D. (2003a). Functionally important calmodulin binding sites in both N- and C-terminal regions of the cone photoreceptor cyclic nucleotide-gated channel CNGB3 subunit. J. Biol. Chem. *278*, 24617–24623.

Peng, C., Rich, E.D., and Varnum, M.D. (2003b). Achromatopsia-associated mutation in the human cone photoreceptor cyclic nucleotide-gated channel CNGB3 subunit alters the ligand sensitivity and pore properties of heteromeric channels. J. Biol. Chem. *278*, 34533–34540.

Picones, A., and Korenbrot, J.I. (1992). Permeation and interaction of monovalent cations with the cGMP-gated channel of cone photoreceptors. J. Gen. Physiol. *100*, 647–673.

Picones, A., and Korenbrot, J.I. (1995). Permeability and interaction of Ca^{2+} with cGMP-gated ion channels differ in retinal rod and cone photoreceptors. Biophys. J. *69*, 120–127.

Rebrik, T.I., and Korenbrot, J.I. (2004). In intact mammalian photoreceptors, Ca^{2+}-dependent modulation of cGMP-gated ion channels is detectable in cones but not in rods. J. Gen. Physiol. *123*, 63–75.

Rho, S., Lee, H.M., Lee, K., and Park, C. (2000). Effects of mutation at a conserved N-glycosylation site in the bovine retinal cyclic nucleotide-gated ion channel. FEBS Lett. *478*, 246–252.

Richards, M.J., and Gordon, S.E. (2000). Cooperativity and cooperation in cyclic nucleotide-gated ion channels. Biochemistry *39*, 14003–14011.

Rosenbaum, T., and Gordon, S.E. (2002). Dissecting intersubunit contacts in cyclic nucleotide-gated ion channels. Neuron *33*, 703–713.

Sakmann, B., and Neher, E. (1983). Single-Channel Recording, 1 ed. (New York: Plenum Press).

Salkoff, L., Baker, K., Butler, A., Covarrubias, M., Pak, M.D., and Wei, A. (1992). An essential 'set' of K^+ channels conserved in flies, mice and humans. Trends Neurosci. *15*, 161–166.

Sautter, A., Zong, X., Hofmann, F., and Biel, M. (1998). An isoform of the rod photoreceptor cyclic nucleotide-gated channel beta subunit expressed in olfactory neurons. Proc. Natl. Acad. Sci. USA *95*, 4696–4701.

Schorge, S., and Colquhoun, D. (2003). Studies of NMDA receptor function and stoichiometry with truncated and tandem subunits. J. Neurosci. *23*, 1151–1158.

Shammat, I.M., and Gordon, S.E. (1999). Stoichiometry and arrangement of subunits in rod cyclic nucleotide-gated channels. Neuron *23*, 809–819.

Shapiro, M.S., and Zagotta, W.N. (1998). Stoichiometry and arrangement of heteromeric olfactory cyclic nucleotide-gated ion channels. Proc. Natl. Acad. Sci. USA *95*, 14546–14551.

Shapiro, M.S., and Zagotta, W.N. (2000). Structural basis for ligand selectivity of heteromeric olfactory cyclic nucleotide-gated channels. Biophys. J. *78*, 2307–2320.

Shen, N.V., and Pfaffinger, P.J. (1995). Molecular recognition and assembly sequences involved in the subfamily-specific assembly of voltage-gated K^+ channel subunit proteins. Neuron *14*, 625–633.

Sundin, O.H., Yang, J.M., Li, Y., Zhu, D., Hurd, J.N., Mitchell, T.N., Silva, E.D., and Maumenee, I.H. (2000). Genetic basis of total colourblindness among the Pingelapese islanders. Nat. Genet. *25*, 289–293.

Varnum, M.D., and Zagotta, W.N. (1996). Subunit interactions in the activation of cyclic nucleotide-gated channels. Biophys. J. *70*, 2667–2679.

Varnum, M.D., Black, K.D., and Zagotta, W.N. (1995a). Molecular mechanism for ligand discrimination of cyclic nucleotide-gated channels. Neuron *15*, 619–625.

Varnum, M.D., Maylie, J., Busch, A., and Adelman, J.P. (1995b). Persistent activation of min K channels by chemical cross-linking. Neuron *14*, 407–412.

Weitz, D., Ficek, N., Kremmer, E., Bauer, P.J., and Kaupp, U.B. (2002). Subunit stoichiometry of the CNG channel of rod photoreceptors. Neuron *36*, 881–889.

Xu, J., Yu, W., Jan, Y.N., Jan, L.Y., and Li, M. (1995). Assembly of voltage-gated potassium channels. Conserved hydrophilic motifs determine subfamily-specific interactions between the alpha-subunits. J. Biol. Chem. *270*, 24761–24768.

Yu, W.P., Grunwald, M.E., and Yau, K.W. (1996). Molecular cloning, functional expression and chromosomal localization of a human homolog of the cyclic nucleotide-gated ion channel of retinal cone photoreceptors. FEBS Lett. *393*, 211–215.

Zheng, J., Trudeau, M.C., and Zagotta, W.N. (2002). Rod cyclic nucleotide-gated channels have a stoichiometry of three CNGA1 subunits and one CNGB1 subunit. Neuron *36*, 891–896.

Zhong, H., Molday, L.L., Molday, R.S., and Yau, K.W. (2002). The heteromeric cyclic nucleotide-gated channel adopts a 3A:1B stoichiometry. Nature *420*, 193–198.

Zhong, H., Lai, J., and Yau, K.W. (2003). Selective heteromeric assembly of cyclic nucleotide-gated channels. Proc. Natl. Acad. Sci. USA *100*, 5509–5513.

Zufall, F., and Munger, S.D. (2001). From odor and pheromone transduction to the organization of the sense of smell. Trends Neurosci. *24*, 191–193.